



This is a repository copy of *Multimillennial incremental slip rate variability of the Clarence fault at the Tophouse Road site, Marlborough Fault System, New Zealand*.

White Rose Research Online URL for this paper:
<http://eprints.whiterose.ac.uk/142880/>

Version: Published Version

Article:

Zinke, R., Dolan, J.F., Rhodes, E.J. orcid.org/0000-0002-0361-8637 et al. (5 more authors) (2019) Multimillennial incremental slip rate variability of the Clarence fault at the Tophouse Road site, Marlborough Fault System, New Zealand. *Geophysical Research Letters*, 46 (2). pp. 717-725. ISSN 0094-8276

<https://doi.org/10.1029/2018GL080688>

© 2018 American Geophysical Union. Reproduced in accordance with the publisher's self-archiving policy.

Reuse

Items deposited in White Rose Research Online are protected by copyright, with all rights reserved unless indicated otherwise. They may be downloaded and/or printed for private study, or other acts as permitted by national copyright laws. The publisher or other rights holders may allow further reproduction and re-use of the full text version. This is indicated by the licence information on the White Rose Research Online record for the item.

Takedown

If you consider content in White Rose Research Online to be in breach of UK law, please notify us by emailing eprints@whiterose.ac.uk including the URL of the record and the reason for the withdrawal request.



eprints@whiterose.ac.uk
<https://eprints.whiterose.ac.uk/>



Geophysical Research Letters

RESEARCH LETTER

10.1029/2018GL080688

Key Points:

- Geomorphic analysis of lidar data and a luminescence dating protocol accurately constrain the offset history of a faulted terrace flight
- Clarence fault incremental slip rates, spanning millennia and multiple earthquakes, varied by a factor of 4–5 since latest Pleistocene time
- Comparison of incremental slip rate variability for the Clarence fault and Awatere fault may suggest coordinated system-level slip behavior

Supporting Information:

- Supporting Information S1
- Figure S1

Correspondence to:

R. Zinke,
rzinke@usc.edu

Citation:

Zinke, R., Dolan, J. F., Rhodes, E. J., Van Dissen, R., McGuire, C. P., Hatem, A. E., et al. (2019). Multimillennial incremental slip rate variability of the Clarence fault at the Tophouse Road site, Marlborough fault system, New Zealand. *Geophysical Research Letters*, 46, 717–725. <https://doi.org/10.1029/2018GL080688>








Received 27 SEP 2018

Accepted 29 NOV 2018

Accepted article online 3 DEC 2018

Published online 29 JAN 2019

Multimillennial Incremental Slip Rate Variability of the Clarence Fault at the Tophouse Road Site, Marlborough Fault System, New Zealand

Robert Zinke¹ , James F. Dolan¹ , Edward J. Rhodes^{2,3} , Russ Van Dissen⁴ , Christopher P. McGuire^{3,5} , Alexandra E. Hatem¹ , Nathan D. Brown^{3,6} , and Robert M. Langridge⁴

¹Department of Earth Sciences, University of Southern California, Los Angeles, CA, USA, ²Department of Geography, University of Sheffield, Sheffield, UK, ³Department of Earth, Planetary, and Space Sciences, University of California, Los Angeles, CA, USA, ⁴GNS Science, Lower Hutt, New Zealand, ⁵Now at School of Geosciences, University of Edinburgh, Edinburgh, UK, ⁶Now at Berkeley Geochronology Center, Berkeley, CA, USA

Abstract Incremental slip rates of the Clarence fault, a dextral fault in the Marlborough fault system of South Island, New Zealand, varied by a factor of 4–5 during Holocene–latest Pleistocene time, as revealed by geomorphic mapping and luminescence dating of faulted fluvial landforms at the Tophouse Road site. We used high-resolution lidar microtopographic data and field surveys to map the fine-scale geomorphology and precisely restore the offset features. We dated the offsets using a stratigraphically informed protocol for infrared stimulated luminescence dating. These data show that incremental slip rates varied from ~2.0 to 9.6 mm/year, averaged over multiple earthquakes and millennial timescales. Comparison to incremental slip rates of the nearby Awatere fault suggests that these faults may behave in coordinated (and anticorrelated) fashion. This study adds to a growing body of evidence suggesting that incremental slip rate variation spanning multiple earthquake cycles may be more common than previously recognized.

Plain Language Summary Faults are commonly assumed to accommodate relative tectonic motions (slip) at constant rates when averaged over several large earthquakes. Testing this assumption requires documenting how far a fault has slipped at several different points in time over the past several millennia. In this study, we examine a rare instance in which four independent markers of fault slip over time are recorded in the landscape along the Clarence fault - a major fault in the Marlborough fault system of South Island, New Zealand. We use high-resolution digital topographic laser scans (lidar) to document the fine-scale topography of the site, and luminescence dating to determine the ages at which the sediments constituting the landforms were last exposed to sunlight. Together, these markers show that, far from being constant over time, the Clarence fault at Tophouse Road has sped up and slowed by by a factor of four or five over the past eleven thousand years or so. This type of study needs to be conducted on other faults to examine whether they have exhibited similar behavior. Such phenomena can provide insights into the processes controlling tectonic plate behavior over timescales of hundreds to thousands of years.

1. Introduction

Fault slip rate data are key to understanding spatiotemporal patterns of earthquake occurrence and the processes governing plate boundary behavior. Furthermore, fault slip rates provide a basic input for most seismic hazard assessment strategies (e.g., Field et al., 2017; Stirling et al., 2012). Emerging evidence suggests that whereas some faults exhibit relatively constant slip rates over time (e.g., Gold & Cowgill, 2011; Kozacı et al., 2009; Salisbury et al., 2018; Van Der Woerd et al., 2002), others undergo periods of accelerated strain release spanning multiple earthquake cycles (e.g., Dolan et al., 2016; Gold & Cowgill, 2011; Mason et al., 2006; Ninis et al., 2013; Wallace, 1987; Weldon et al., 2004; Zinke et al., 2017). Constraining the incremental slip history of a fault requires a relatively rare set of geologic conditions (i.e., multiple progressively offset features sharing a common kinematic history). Thus, the ability to assess whether faults commonly exhibit episodes of elevated strain release has been severely limited by the number of data available.

In this study, we precisely constrain the incremental slip history of the right-lateral Clarence fault at Tophouse Road, northeastern South Island, New Zealand. Specifically, we use lidar microtopographic maps and field

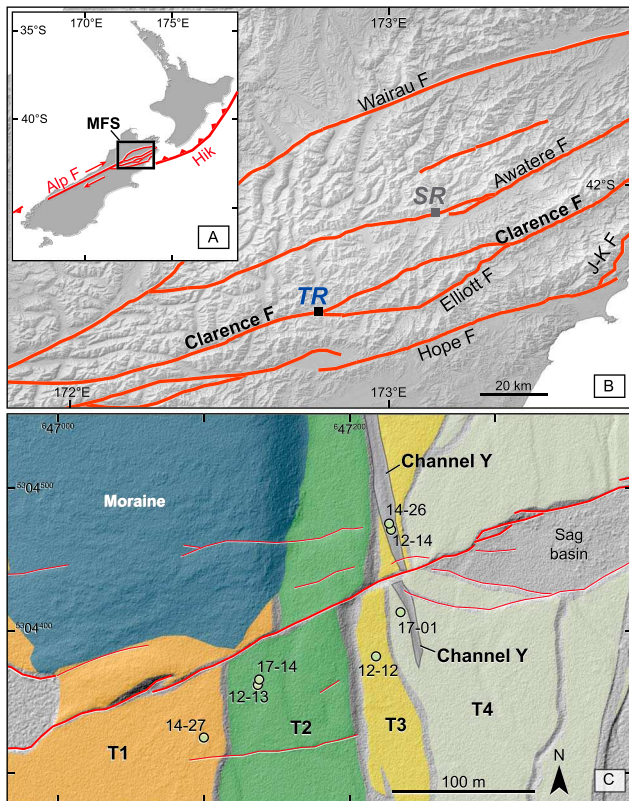


Figure 1. (a) The Marlborough fault system (MFS) transfers slip between the Hikurangi subduction zone (Hik) and Alpine fault (Alp F). (b) Major faults of the (MFS). J-K F is the Jordan-Kekerengu fault system. The Tophouse Road site (TR) is at the western edge of the Clarence-Elliott fault junction (Langridge et al., 2016). SR is the Saxton River site on the Awatere fault. Topography is shown by the Advanced Spaceborne Thermal Emission and Reflection Radiometer Global Digital Elevation Model. (c) Geomorphic surfaces mapped on hillshaded lidar. Thick red line is the primary fault trace; thin red lines are secondary faults. Green dots are sample pits, labeled by pit number.

data to accurately measure fault displacements recorded by a series of progressively offset fluvial landforms and employ a stratigraphically informed luminescence dating protocol to date the landforms. From these measurements, we determine the incremental slip rates of the Clarence fault spanning Holocene and latest Pleistocene time. Finally, we discuss the implications of the observed temporal strain release patterns in relation to the use of geologic slip rates in active tectonic studies and seismic hazard assessment.

2. The Tophouse Road Site, Clarence Fault

The Clarence fault is one of the four principal dextral strike-slip faults within the Marlborough fault system (MFS) of northern South Island, New Zealand. Together, these faults accommodate most of the relative Pacific-Australian plate boundary motion between the Hikurangi subduction margin and the Alpine fault (Figure 1; Van Dissen & Yeats, 1991; Wallace et al., 2012; Litchfield et al., 2014). The Tophouse Road site is located at the western edge of the junction between the Clarence and Elliott faults, where the Clarence fault crosses the western bank of the southward flowing Clarence River (Kieckhefer, 1979; Knuepfer, 1992). The site comprises a series of faulted and progressively offset fluvial terrace risers and channels that provide ideal piercing lines for offset restoration.

The fluvial depositional history of the Tophouse Road site began during latest Pleistocene time when glacial outwash gravels aggraded throughout the upper Clarence River Valley, buttressing a large glacial moraine that bounds the western edge of the site and forming the T1 floodplain (Figure 1c; Bull & Knuepfer, 1987; Knuepfer, 1992). As sediment supply waned, the Clarence River incised into T1, eventually isolating the T1 terrace tread from further river occupation. Further episodes of incision and floodplain stability led to the formation of younger terrace treads (T2–T4; Figure 1c) separated by steep terrace risers, denoted here as the tread names separated by a slash (e.g., T1/T2 riser). Periods of high-energy streamflow, during which Clarence River streampower was sufficient to laterally trim the adjacent risers, are consistent with coarse-grained, pebble-boulder gravels and sand deposits (Bull & Knuepfer, 1987; Cowgill, 2007;

Lensen, 1964; Mason et al., 2006; Zinke et al., 2017). The gravels and sands are typically capped by younger silt horizons, which represent (1) the waning stages of terrace occupation, (2) overbank deposits from younger floodplains, and/or (3) loess. In any of these cases, the silt deposits represent periods of low-energy streamflow (or no flow at all) that was incapable of significantly modifying terrace risers or channel geometries. Remnant channel morphologies are discernable within several of the terraces. Notably, “Channel Y” cross-cuts both the T3 and T4 terraces (Figure 1), as discussed below.

3. Offset Measurements

Our geomorphic mapping of the Tophouse Road offsets builds on air photo- and field-based interpretations by Kieckhefer (1979) and Knuepfer (1992). Here we use lidar microtopographic data (Figures 1 and 2 and supporting information Figures S1 and S2; Dolan & Rhodes, 2016) and field observations to precisely document the cumulative offset recorded by four dateable offset geomorphic features: (1) the T1/T2 terrace riser; (2) the T2/T3 riser; (3) the T3/T4 riser; and (4) Channel Y. To measure each offset using the lidar data, we backslipped one side of the feature relative to the other and visually determined a preferred (most likely) displacement value. Our reported uncertainties represent the maximum and minimum limits of sedimentologically allowable geometries (Figure S3). In our slip rate calculations, we expressed our offset restoration values as triangular or trapezoidal-shaped probability density functions.

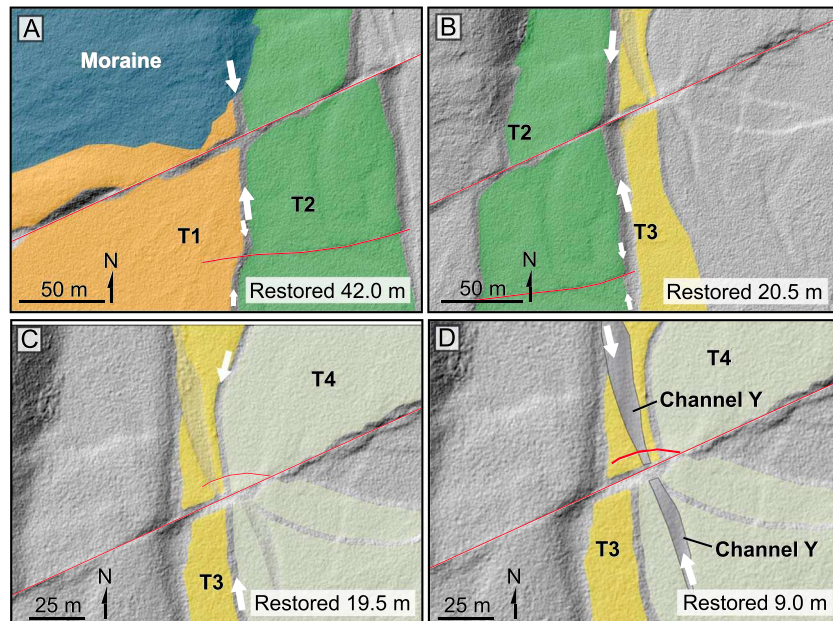


Figure 2. Offset markers restored to their preferred values across primary fault strand (see Figure S3). White arrows indicate the primary feature restored. (a) T1/T2 riser. A secondary, southern fault strand accounts for an additional ~ 5 m of slip (small white arrows; Figure S3a). (b) T2/T3 riser. The southern secondary fault accommodates an additional ~ 1 m of slip (Figure S3b). (c) T3/T4 riser. Curved red line is the northern boundary of a pop-up structure that may disrupt near-fault riser geometry. (d) Channel Y.

The T1/T2 riser is topographically sharp and linear across the primary fault, allowing for precise right-lateral offset determination of $42.0 + 2.0/-1.5$ m (Figures 2a and S3A). Additionally, a secondary fault strand cuts the T1/T2 riser ~ 70 m south of the main fault (Figure S3e). This strand accommodates $5.0 + 1.0/-1.5$ m of fault slip, yielding a total of 47.0 ± 3.0 m of right-lateral slip.

The T2/T3 riser is defined by a gentle, continuous curve within a ~ 40 -m width on either side of the primary fault, bounded by a backedge channel at the base of the riser. Our reconstructions restore the broad, smooth curvature of the riser, resulting in a geometry similar to those of other channels within the active Clarence River floodplain to the east. This yielded a right-lateral offset of 20.5 ± 1.5 m (Figures 2b and S3b). The secondary strand to the south accommodates 1.0 ± 0.5 m of fault slip. Adding this additional offset yields a total right-lateral offset of 21.5 ± 2.0 m.

Uncertainty in projecting the T3/T4 riser into the fault stems from whether or not the riser is coherent and discernable across a ~ 15 -m-wide pop-up structure immediately north of the fault (Figures 2c and S3c). If the riser is continuous and uninterrupted (i.e., not horizontally displaced) across this feature, our preferred restoration is 21.5 ± 0.5 m (the same as the T2/T3 offset). Alternatively, the pop-up might disrupt the near-fault geometry of the riser (e.g., by accommodating antithetic shear and clockwise rotation). If so, our preferred restoration is 17.5 ± 0.5 m. Because we consider these interpretations equally valid, we describe the riser offset using a trapezoid-shaped probability distribution, with a uniform “boxcar” from 17.5–21.5 m and probabilities diminishing to 0 at the extreme ends (17.0 and 22.0 m).

After high-energy flow (capable of transporting gravel bedload) across the T4 floodplain ceased, Channel Y formed as a minor offshoot of the Clarence River due to river avulsion further north (details in Figure S3f). It cross-cuts T3 and T4 (Figures 2d and S3). The northern and southern reaches of Channel Y restore to 9.0 ± 1.0 m right-lateral offset.

4. Age Determinations

We dated the landforms at Tophouse Road using a sedimentologically informed protocol for infrared stimulated luminescence (IRSL) dating (Text S4). We excavated seven pits into the Tophouse Road terraces and

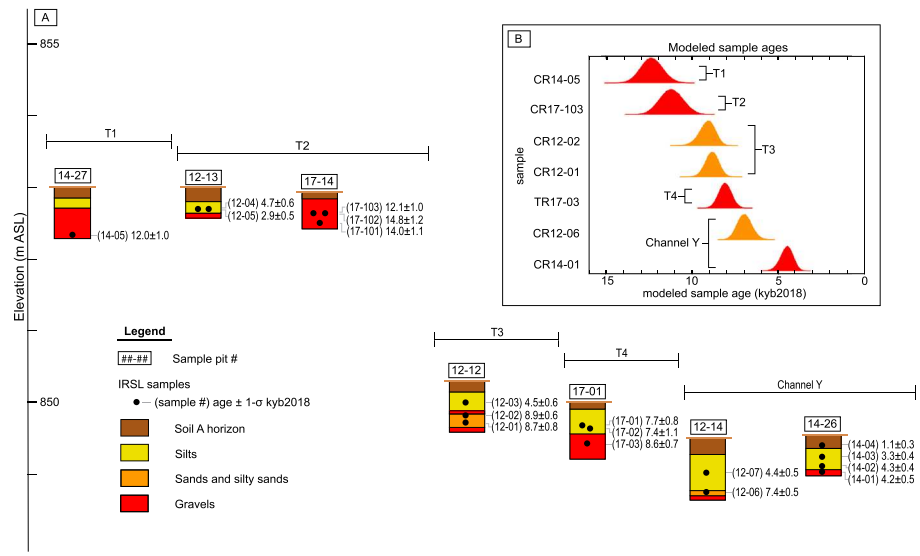


Figure 3. (a) Morphostratigraphic diagram of sample pits and ages relative to elevation (m) and corresponding geomorphic surfaces. Because pits were excavated at slightly different distances from the fault on gently south sloping terrace surfaces (Figure 1), apparent relative vertical positions do not necessarily reflect terrace heights at the fault. (b) Modeled gravel and sand samples ages from step 2 of our age model (Text S4).

channels, in which we logged the stratigraphy and collected samples for dating (Figures 1c and 3a). In all, we collected and dated 18 samples using the post-IR-IRSL₂₂₅ single K-feldspar grain procedure of Rhodes (2015), and Lewis et al. (2017; see also Huntley & Baril, 1997). The ages are reported in thousands of years before 2018 (kyb2018). We used a two-step Bayesian age model (based on OxCal 4.3; Bronk Ramsey, 2001, 2017; Rhodes et al., 2003; Zinke et al., 2017; Text S4) to refine the terrace and channel ages based on stratigraphic observations. The first step of our age model trimmed the gravel and silt ages in each pit according to their lithostratigraphic ordering. For example, knowledge that the silts in Pit 17-01 are stratigraphically higher and younger than the gravels allowed us to trim the gravel sample age. Step 2 of our age model accounts for the morphologic information that lower terraces are sequentially younger than higher ones, and the cross-cutting Channel Y is younger than the treads into which it is incised. In this step, we included only the gravel and sand ages representing high-energy river occupation of the terrace floodplain or channelized streamflow (Figure 3b). We averaged samples CR12-01 and CR12-02 in Pit 12-12 based on their similar ages and stratigraphic context. We refer to poststep 2 ages as “modeled ages.”

5. Slip Rate Determinations

To reconstruct the incremental slip history of the Clarence fault at Tophouse Road, we dated each offset geomorphic feature by considering its relation to the dated stratigraphic units at the site (e.g., Zinke et al., 2017). We evaluated whether the upper or lower terrace age is more appropriate to date each offset marker by considering its morphological and sedimentological context (Cowgill, 2007; Lensen, 1964). The offsets, ages, and slip rates are tabulated in Table S7.

The T1/T2 morphology is sharply defined and similar on either side of the fault, showing no evidence of a diachronous origin (see Gold et al., 2009), as would have resulted from inefficient lateral trimming by the Clarence River. This morphology instead implies that any fault offset was effectively removed by the river until abandonment of the lower T2 floodplain, as might be expected considering that high-energy streamflow across T2 was capable of transporting the cobble-boulder bedload of the T2 floodplain. We therefore use the modeled T2 abandonment age of 11.2 ± 1.3 kyb2018 (2-sigma confidence, based on sample CR17-103) to date the T1/T2 riser offset (47.0 ± 3.0 m).

The T2/T3 riser is bounded by a backedge channel within the T3 surface. In its restored configuration (Figure 2b), the riser was trimmed by channelized flow along the back edge of the T3 floodplain during high-energy stages of streamflow across T3. Thus, the coarse-grained sand deposits dating T3

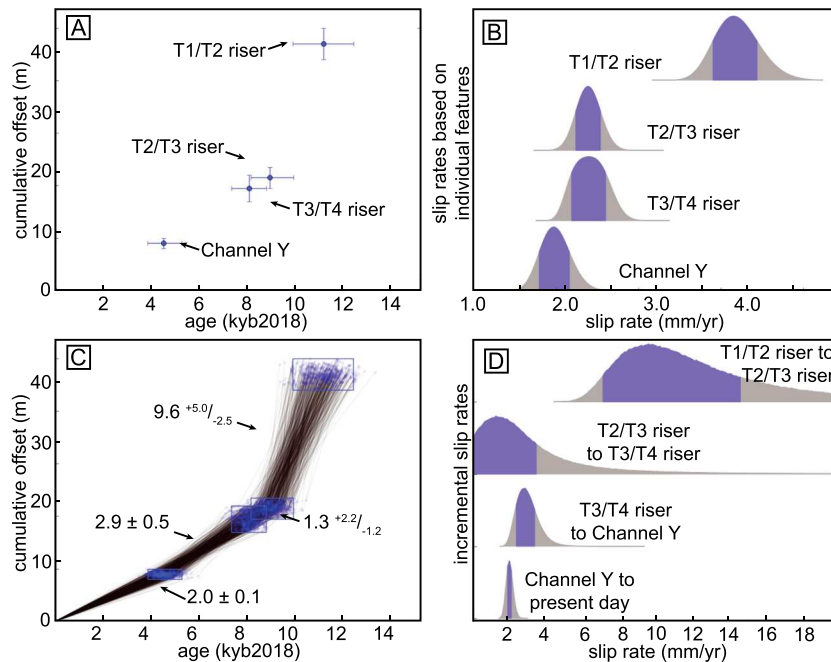


Figure 4. Displacement-age history of the Clarence fault at Tophouse Road. (a) Offset and age determinations for geomorphic features (preferred values and 95% confidence limits). (b) Relative probability of slip rates averaged since present day for each marker. Blue fields show highest 68.27% probability. (c) Monte Carlo sampling of offset and age distributions (blue boxes as in (a)). Labels are incremental slip rates. (d) Incremental slip rate probability density functions (blue fields as in (b)). The T2/T3 to T3/T4 riser interval appears truncated at 0 because there is a significant probability that no slip occurred during this time.

abandonment also date the end of T2/T3 trimming. The T3 backedge channel may have sustained minor streamflow after this time, but any such flow did not significantly erode the T2/T3 riser north of the fault, based on the smooth, continuous curvature of the restored riser. The T2/T3 riser therefore records 21.5 ± 2.0 m of offset since $9.0 + 1.0/-0.9$ kyb2018 (based on samples CR12-01 and CR12-02).

The T3/T4 riser offset ($17.5-21.5 \pm 0.5$ m) is dated by the youngest bedload gravel deposits of T4, which mark the end of high-energy streamflow across the T4 floodplain. Sample TR17-03 dates these gravel deposits, yielding a modeled age of $8.1 + 0.8/-0.7$ kyb2018.

Channel Y cross-cuts the T3 and T4 terraces and therefore postdates high-energy river occupation of those surfaces. We excavated two pits into the Channel Y deposits, revealing silt overlying sands and gravels at $\sim 50-75$ cm below the present-day ground surface (Figures 1 and 3). The youngest gravel sample from these pits represents the most recent age at which streamflow was sufficiently high energy to erode and modify the channel geometry. We therefore use the $4.5 + 0.8/-0.7$ kyb2018 modeled age of gravel sample CR14-01 to date the 9.0 ± 1.0 m of slip recorded by Channel Y.

These four dated, offset geomorphic markers constrain the incremental displacement-time history of the Clarence fault at Tophouse Road (Figure 4a). We first calculated the slip rate recorded by each individual feature, averaged since the time of marker formation to the present day (Figure 4b) by convolving the offset and age probability density functions (using the formulation of Bird, 2007). These slip rates and associated 68.27% uncertainties are the following: $4.2 + 0.2/-0.3$ mm/year (T1/T2 riser), $2.4 + 0.1/-0.2$ mm/year (T2/T3 riser), 2.4 ± 0.2 mm/year (T3/T4 riser), and 2.0 ± 0.2 mm/year (Channel Y).

We also determined the incremental slip rates between different offset markers to show how slip rate varied over different time periods (Figures 4c and 4d). We achieved this using a Monte Carlo sampling approach, in which physically realistic incremental slip rate estimates were obtained by rejecting sample paths resulting in negative (left-lateral) slip rates (Gold & Cowgill, 2011; Zinke et al., 2017; Text S5 and Python Script S6). The displacement-time markers at Tophouse Road characterize slip rates over four distinct intervals. First, from circa 11.2–9.0 ka the Clarence fault slipped at an average rate of $9.6 + 5.0/-2.5$ mm/year (Figure 4d),

sustained over ~ 25.5 m of slip. Second, for a relatively brief period between circa 9.0–8.1 ka, the fault may have experienced ~ 3 –4 m of slip or may not have experienced any surface-rupturing earthquakes. Specifically, if our ~ 21.5 -m offset estimate for the T3/T4 riser is correct, then the Clarence fault at Tophouse Road experienced a seismic lull between the age of the T3/T4 riser (ca. 8.1 ka) and the age of the T2/T3 riser (ca. 9.0 ka), which is offset by the same amount. Alternatively, if our estimate of ~ 17.5 m is correct, then the Clarence fault experienced ~ 4 m of surface slip—possibly one large event—over this time. Making no assumptions about which case is correct (i.e., allowing the slip rate to range between 0 and infinity over this short interval) yields an incremental slip rate of $1.3 + 2.2/-1.2$ mm/year. More recently, during the third interval spanning circa 8.1–4.5 ka, the Clarence fault slipped at a relatively slow rate of 2.9 ± 0.5 mm/year. Finally, the fault slip rate has been similarly slow since circa 4.5 ka to the present, averaging 2.0 ± 0.2 mm/year. Although variations in the timing and displacement of earthquakes within each interval may have produced finer-scale slip rate variations, our results nevertheless allow us to assess fundamental temporal patterns of fault slip rate variability over periods spanning multiple earthquake cycles.

6. Discussion and Conclusions

The incremental slip history of the Clarence fault at Tophouse Road is marked by significant (factor of 4–5) variations in incremental slip rate, sustained over periods spanning thousands of years (~ 1 –4 kyr) and meters or tens of meters of slip (~ 4 –25 m) during Holocene and latest Pleistocene time. As detailed above, the incremental slip history of the Clarence fault at Tophouse Road can be characterized as relatively fast during latest Pleistocene and early Holocene time (ca. 11.2–9.0 ka), followed by a transitional period, and finally a period of relatively slow strain release since mid-Holocene time (ca. 8.1 ka).

The Tophouse Road site presents an ideal opportunity to study incremental slip rate variability in which all offset markers come from a single, ~ 300 -m-long stretch of the fault and can confidently be assumed to share a common tectonic history without the need to combine features from different sites (e.g., Gold & Cowgill, 2011). Although we note the presence of a small sag basin at the eastern edge of the site, it is unlikely that deformation associated with this feature significantly influenced our slip rate measurements, as the features upon which we based our offset measurements do not appear to bend into the fault (Figure 1c). We also note that the site is on the western edge of a transfer zone between Clarence and Elliott faults (Figure 1b). However, because the mapped surface trace of the Elliott fault ends ~ 2 km to the southeast (Langridge et al., 2016), the proportion of strain localized on the main fault should be similar across the site.

Slip rate data such as these provide crucial constraints on the likely tectonic processes controlling plate boundary deformation, as they result from interactions between the physical properties of the fault zone and lithospheric stresses. For instance, alternating cycles of strain hardening and weakening of fault zone rocks could lead to seismic lulls and clusters of earthquake activity (Chéry & Vernant, 2006; Dolan et al., 2007, 2016; Oskin et al., 2008). These effects could be especially pronounced if crustal rocks act as an “elastic strain capacitor” (Dolan et al., 2016; Fay & Humphreys, 2006), storing more elastic strain than is released in a single event, then releasing that stored energy in an earthquake cluster (Dolan et al., 2016; Sieh et al., 2008; Weldon et al., 2004).

At the broadest spatial scales, plate boundary faults are driven by relative tectonic plate motion. Although these motions are generally assumed to be constant over million-year timescales (e.g., DeMets et al., 2010), shorter-term variations (due to, e.g., subduction earthquakes) may be masked within the temporal resolution of the record (Anderson, 1975; Meade & Loveless, 2017). In contrast, at the most local, short-term spatiotemporal scales, interevent coordination between heterogeneously stressed fault patches may lead to phases of increased earthquake activity, including anomalously large displacements in some events (e.g., Barbot et al., 2012; Cisternas et al., 2005; Konca et al., 2008). However, these effects are likely most important over time and displacement scales spanning one to several earthquakes and cannot explain the longer-term patterns of slip rate variability observed at Tophouse Road.

Between these end-member time and length scales may operate a host of different processes controlling rates of strain accumulation and release. These include climate-driven processes such as changes in glacial loading (Hetzl & Hampel, 2005) and eustatic sea level changes (Luttrell & Sandwell, 2010), as well as interactions between faults in mechanically complementary fault networks (Loveless & Meade, 2011; Sammis et al., 2003; Scholz, 2010). Considering the location of the Clarence fault within the MFS (Figure 1), one might expect

earthquake activity along nearby faults to influence Clarence fault behavior. Interestingly, the extreme slip rate variability observed at Tophouse Road is similar in magnitude and duration to that on the Awatere fault at Saxton River (Zinke et al., 2017). The periods of relatively “fast” and “slow” slip on these faults, however, appear to be anticorrelated in time: While the Clarence fault at Tophouse Road was experiencing a rapid slip rate between 11 and 9 ka, the Awatere fault at Saxton River was moving relatively slowly, and when the Clarence fault at Tophouse Road slowed down following circa 8 ka, the Awatere fault at Saxton River sped up. Although reliable incremental slip rate data along the nearby Wairau and Hope faults are forthcoming (Hatem et al., 2016), these observations hint at potentially coordinated system-level behavior in which the major strike-slip faults of the MFS trade slip in time and space.

Regardless of the cause, the striking differences in incremental slip rate during the fast and slow periods at Tophouse Road illustrate the need for caution when using only a single slip rate marker for geologic and geodetic fault studies and seismic hazard assessment. For instance, geologically determined fault slip rates and geodetically inferred slip deficit rates (i.e., “geodetic slip rates”) are often compared to assess the role of faults in accommodating strain across a region. Geologic slip rates based on a single marker formed during a slow period (such as that between present day and ca. 8 ka at Tophouse Road) may be significantly slower than the geodetic slip deficit rate (e.g., Dolan et al., 2016; Dolan & Meade, 2017). Without further evidence, this may lead one to conclude that either (1) the fault plays a relatively minor role in accommodating the total strain across the region (e.g., England & Molnar, 2005) or (2) a significant amount of strain across the fault is accommodated as distributed, off-fault deformation unaccounted for in the offset restoration (e.g., Dolan & Haravitch, 2014; Hergert & Heidbach, 2010; Milliner et al., 2016; Zinke et al., 2015). Conversely, if the slip rate marker formed during a fast period (e.g., between ca. 11 and 9 ka at Tophouse Road), the geologic rate may overestimate the geodetic slip deficit rate. This may lead one to infer extreme earthquake cycle effects (e.g., Dolan & Meade, 2017) or variations in the strength of lithospheric rocks (e.g., Dolan et al., 2007, 2016; Dolan & Meade, 2017). Similarly, the unknowing use of a slip rate representing a slow period in a seismic hazard assessment may result in an underestimate of the hazard posed by a fault, whereas use of a slip rate from a fast period may overestimate the hazard. More incremental slip rate data like those presented above are required to properly quantify the prevalence and magnitude of slip rate variability on faults worldwide.

These observations raise the following question: Over what time and displacement scales do incremental slip rates reflect their “average,” long-term rate? Put another way, is there a characteristic amount of slip or time over which the variations in slip rate average out? The incremental slip rate data we present here give no indication that the Clarence fault has reached a consistent average rate over the total time (~11 kyr) and displacement (~47 m) recorded at Tophouse Road. Instead, even larger-displacement and longer-term data could be necessary, and these values may depend on the specific properties of the fault in question (e.g., tectonic setting, slip rate, and structural maturity). Further development of high-resolution incremental slip rate records such as the one presented here may shed light on these questions.

Acknowledgments

This research was funded by U.S. National Science Foundation grants EAR-1321914 (Dolan) and EAR-1321912 (Rhodes) and by GNS Science. Our manuscript benefitted from reviews by Tim Little and an anonymous reviewer. We thank Michael Say, Shawn Lu, Marina Argueta, Joel Davies, and Rob Ashurst for sample preparation; Jess Grenader for field assistance; and Neil Fowke and N.Z. Department of Conservation for permitting assistance. Data used in this study conform to AGU policy and can be found in the supporting information (Figures S1–S3, Texts S4 and S5, Python Script S6, and Table S7).

References

- Anderson, D. L. (1975). Accelerated plate tectonics. *Science*, *187*(4181), 1077–1079. <https://doi.org/10.1126/science.187.4181.1077>
- Barbot, S., Lapusta, N., & Avouac, J.-P. (2012). Under the hood of the earthquake machine: Toward predictive modeling of the seismic cycle. *Science*, *336*(6082), 707–710. <https://doi.org/10.1126/science.1218796>
- Bird, P. (2007). Uncertainties in long-term geologic offset rates of faults: General principles illustrated with data from California and other western states. *Geosphere*, *3*(6), 577–595. <https://doi.org/10.1130/GES00127.1>
- Bronk Ramsey, C. (2001). Development of the radiocarbon program OxCal. *Radiocarbon*, *43*(2A), 355–363. <https://doi.org/10.1017/S0033822200038212>
- Bronk Ramsey, C. (2017). OxCal program, version 4.3.
- Bull, W. L., & Knuepfer, P. L. K. (1987). Adjustments by the Charwell River, New Zealand, to uplift and climatic changes. *Geomorphology*, *1*(1), 15–32. [https://doi.org/10.1016/0169-555X\(87\)90004-3](https://doi.org/10.1016/0169-555X(87)90004-3)
- Chéry, J., & Vernant, P. (2006). Lithospheric elasticity promotes episodic fault activity. *Earth and Planetary Science Letters*, *243*(1–2), 211–217. <https://doi.org/10.1016/j.epsl.2005.12.014>
- Cisternas, M., Atwater, B. F., Torrejón, F., Sawai, Y., Machuca, G., Lagos, M., et al. (2005). Predecessors of the giant 1960 Chile earthquake. *Nature*, *437*(7057), 404–407. <https://doi.org/10.1038/nature03943>
- Cowgill, E. (2007). Impact of riser reconstructions on estimation of secular variation in rates of strike-slip faulting: Revisiting the Cherchen River site along the Altyn Tagh fault, NW China. *Earth and Planetary Science Letters*, *254*(3–4), 239–255. <https://doi.org/10.1016/j.epsl.2006.09.015>
- DeMets, C., Gordon, R. G., & Argus, D. F. (2010). Geologically current plate motions. *Geophysical Journal International*, *181*(1), 1–80. <https://doi.org/10.1111/j.1365-246X.2009.04491.x>

- Dolan, J. F., Bowman, D. D., & Sammis, C. G. (2007). Long-range and long-term fault interactions in Southern California. *Geology*, *35*(9), 855–858. <https://doi.org/10.1130/G23789A.1>
- Dolan, J. F., & Haravitch, B. D. (2014). How well do surface slip measurements track slip at depth in large strike-slip earthquakes? The importance of fault structural maturity in controlling on-fault slip versus off-fault surface deformation. *Earth and Planetary Science Letters*, *388*, 38–47. <https://doi.org/10.1016/j.epsl.2013.11043>
- Dolan, J. F., McAuliffe, L. J., Rhodes, E. J., McGill, S. F., & Zinke, R. (2016). Extreme multi-millennial slip rate variations on the Garlock fault, California: Strain super-cycles, potentially time-variable fault strength, and implications for system-level earthquake occurrence. *Earth and Planetary Science Letters*, *445*, 79–91. <https://doi.org/10.1016/j.epsl.2016.04.001>
- Dolan, J. F., & Meade, B. J. (2017). A comparison of geodetic and geologic rates prior to large strike-slip earthquakes: A diversity of earthquake-cycle behaviors? *Geochemistry, Geophysics, Geosystems*, *18*, 4426–4436. <https://doi.org/10.1002/2017GC007014>
- Dolan, J. F., & Rhodes, E. J. (2016). *Marlborough fault system*. South Island, New Zealand: National Center for Airborne Laser Mapping. Retrieved from <http://opentopography.org>, <https://10.5069/G9G44N75>
- England, P., & Molnar, P. (2005). Late Quaternary to decadal velocity fields in Asia. *Journal of Geophysical Research*, *110*(B12). <https://doi.org/10.1029/2004JB003541>
- Fay, N., & Humphreys, E. (2006). Dynamics of the Salton block: Absolute fault strength and crust-mantle coupling in Southern California. *Geology*, *34*(4), 261–264. <https://doi.org/10.1130/G22172.1>
- Field, E. H., Jordan, T. H., Page, M. T., Milner, K. R., Shaw, B. E., Dawson, T. E., et al. (2017). A Synoptic View of the Third Uniform California Earthquake Rupture Forecast (UCERF3). *Seismological Research Letters*, *88*(5), 1259–1267. <https://doi.org/10.1785/0220170045>
- Gold, R. D., & Cowgill, E. (2011). Deriving fault-slip histories to test for secular variation in slip, with examples from the Kunlun and Awatere faults. *Earth and Planetary Science Letters*, *301*(1–2), 52–64. <https://doi.org/10.1016/j.epsl.2010.10.011>
- Gold, R. D., Cowgill, E., Arrowsmith, J. R., Gosse, J., Chen, X., & Wang, X.-F. (2009). Riser diachroneity, lateral erosion, and uncertainty in rates of strike-slip faulting: A case study from Tuzidun along the Altyn Tagh fault, NW China. *Journal of Geophysical Research*, *114*, B04401. <https://doi.org/10.1029/2008JB005913>
- Hatem, A. E., Dolan, J. F., Langridge, R. M., Zinke, R. W., McGuire, C. P., Rhodes, E. J., & Van Dissen, R. J. (2016). Incremental slip rate and paleoseismic data from the eastern Hope fault, New Zealand: The Hossack and Green Burn sites. Abstract T32B-07 Presented at EOS Transactions of the AGU, Fall Annual AGU Meeting, San Francisco, CA, December 12.
- Hergert, T., & Heidbach, O. (2010). Slip-rate variability and distributed deformation in the Marmara Sea fault system. *Nature Geoscience*, *3*(2), 132–135. <https://doi.org/10.1038/ngeo739>
- Hetzl, R., & Hampel, A. (2005). Slip rate variations on normal faults during glacial-interglacial changes in surface loads. *Nature*, *435*(7038), 81–84. <https://doi.org/10.1038/nature03562>
- Huntley, D. J., & Baril, M. (1997). The K content of the K-feldspar being measured in optical dating or in thermoluminescence dating. *Ancient TL*, *15*, 11–13.
- Kieckhefer, R. M. (1979). Sheets M31D, N31A, N31C and pts M32A & M32B. Leader Dale. In *Late Quaternary tectonic map of New Zealand 1:50,000*, (1st ed.). Wellington, New Zealand: Department of Scientific and Industrial Research.
- Knuepfer, P. L. K. (1992). Temporal variations in latest Quaternary slip across the Australian-Pacific plate boundary, northeastern South Island, New Zealand. *Tectonics*, *11*(3), 449–464. <https://doi.org/10.1029/91TC02890>
- Konca, A. O., Avouac, J.-P., Sladen, A., Meltzner, A. J., Sieh, K., Fang, P., et al. (2008). Partial rupture of a locked patch of the Sumatra megathrust during the 2007 earthquake sequence. *Nature*, *456*(7222), 631–635. <https://doi.org/10.1038/nature07572>
- Kozacı, O., Dolan, J. F., & Finkel, R. C. (2009). A late Holocene slip rate for the central north Anatolian fault, at Tahtaköprü, Turkey, from cosmogenic ¹⁰Be geochronology: Implications for fault loading and strain release rates. *Journal of Geophysical Research*, *114*, B01405. <https://doi.org/10.1029/2008JB005760>
- Langridge, R. M., Ries, W. F., Litchfield, N. J., Villamor, P., Van Dissen, R. J., Rattenbury, M. S., et al. (2016). The New Zealand active faults database: NZAFD250. *New Zealand Journal of Geology and Geophysics*, *59*(1), 86–96. <https://doi.org/10.1080/00288306.2015.1112818>
- Lenssen, G. J. (1964). The general case of progressive fault displacement of flights of degradational terraces. *New Zealand Journal of Geology and Geophysics*, *7*(4), 871–876. <https://doi.org/10.1080/00288306.1964.10428135>
- Lewis, C. J., Sancho, C., McDonald, R. V., Peña-Monné, J. L., Puevo, E. L., Rhodes, E. J., et al. (2017). Post-tectonic landscape evolution in NE Iberia using a staircase of terraces: Combined effects of uplift and climate. *Geomorphology*, *292*, 85–103. <https://doi.org/10.1016/j.geomorph.2017.04.037>
- Litchfield, N. J., Van Dissen, R., Sutherland, R., Barnes, P. M., Cox, S. C., Norris, R., et al. (2014). A model of active faulting in New Zealand. *New Zealand Journal of Geology and Geophysics*, *57*(1), 32–56. <https://doi.org/10.1080/00288306.2013.854256>
- Loveless, J. P., & Meade, B. J. (2011). Stress modulation on the San Andreas fault by interseismic fault system interactions. *Geology*, *39*(11), 1035–1038. <https://doi.org/10.1130/G32215.1>
- Luttrell, K., & Sandwell, D. (2010). Ocean loading effects on stress at near shore plate boundary fault systems. *Journal of Geophysical Research*, *115*, B08411. <https://doi.org/10.1029/2009JB006541>
- Mason, D. P. M., Little, T. A., & Van Dissen, R. J. (2006). Rates of active faulting during late Quaternary fluvial terrace formation at Saxton River, Awatere fault, New Zealand. *Geological Society of America Bulletin*, *118*(11–12), 1431–1446. <https://doi.org/10.1130/B25961.1>
- Meade, B. J., & Loveless, J. P. (2017). Block motion changes in Japan triggered by the 2011 great Tohoku earthquake. *Geochemistry, Geophysics, Geosystems*, *18*, 2459–2466. <https://doi.org/10.1002/2017GC006983>
- Milliner, C. W. D., Dolan, J. F., Hollingsworth, J., Leprince, S., & Ayoub, F. (2016). Comparison of coseismic near-field and off-fault surface deformation patterns of the 1992 M_w 7.3 Landers and 1999 M_w 7.1 Hector Mine earthquakes: Implications for controls on the distribution of surface strain. *Geophysical Research Letters*, *43*, 10,115–10,124. <https://doi.org/10.1002/2016GL069841>
- Ninis, D., Little, T. A., Van Dissen, R. J., Litchfield, N. J., Smith, E. G. C., Wang, N., et al. (2013). Slip rate on the Wellington fault, New Zealand, during the Late Quaternary: Evidence for variable slip during the Holocene. *Bulletin of the Seismological Society of America*, *103*(1), 559–579. <https://doi.org/10.1785/0120120162>
- Oskin, M., Perg, L., Shelef, E., Strane, M., Gurney, E., Singer, B., & Zhang, X. (2008). Elevated shear zone loading rate during an earthquake cluster in eastern California. *Geology*, *36*(6), 507–510. <https://doi.org/10.1130/G24814A.1>
- Rhodes, E. J. (2015). Dating sediments using potassium feldspar single-grain IRSL: Initial methodological considerations. *Quaternary International*, *362*, 14–22. <https://doi.org/10.1016/j.quaint.2014.12.012>
- Rhodes, E. J., Bronk-Ramsey, C., Outram, Z., Batt, C., Willis, L., Dockrill, S., & Bond, J. (2003). Bayesian methods applied to the interpretation of multiple OSL dates: High precision sediment age estimates from old Scatness Broch excavations, Shetland Isles. *Quaternary Science Reviews*, *22*(10–13), 1231–1244. [https://doi.org/10.1016/S0277-3791\(03\)00046-5](https://doi.org/10.1016/S0277-3791(03)00046-5)

- Salisbury, J. B., Arrowsmith, J. R., Brown, N., Rockwell, T., Akciz, S., & Grant Ludwig, L. (2018). The age and origin of small offsets at Van Matre Ranch along the San Andreas fault in the Carrizo plain, California. *Bulletin of the Seismological Society of America*, 108(2), 639–653. <https://doi.org/10.1785/0120170162>
- Sammis, C. G., Dolan, J. F., Smith, S. W. (2003). Phase-locking in coupled non-linear relaxation oscillators: An explanation for observed temporal and spatial correlation and anti-correlation of large earthquakes. EOS: Transactions of the American Geophysical Union 84 (46) (Fall Meeting Supplemental Abstract NG32A-07)
- Scholz, C. H. (2010). Large earthquake triggering, clustering, and the synchronization of faults. *Bulletin of the Seismological Society of America*, 100(3), 901–909. <https://doi.org/10.1785/0120090309>
- Sieh, K., Natawidjaja, D. H., Meltzner, A. J., Shen, C.-C., Cheng, H., Li, K.-S., et al. (2008). Earthquake supercycles inferred from sea-level changes recorded in the corals of west Sumatra. *Science*, 322(5908), 1674–1678. <https://doi.org/10.1126/science.1163589>
- Stirling, M., McVerry, G., Gerstenberger, M., Litchfield, N., Van Dissen, R., Berryman, K., et al. (2012). National Seismic Hazard Model for New Zealand: 2010 Update. *Bulletin of the Seismological Society of America*, 102(4), 1514–1542. <https://doi.org/10.1785/0120110170>
- Van Der Woerd, J., Tapponnier, P., Ryerson, F. J., Meriaux, A.-S., Meyer, B., Gaudemer, Y., et al. (2002). Uniform postglacial slip-rate along the central 600 km of the Kunlun fault (Tibet), from ^{26}Al , ^{10}Be , and ^{14}C dating of riser offsets, and climatic origin of the regional morphology. *Geophysical Journal International*, 148(3), 356–388. <https://doi.org/10.1046/j.1365-246x.2002.01556.x>
- Van Dissen, R., & Yeats, R. S. (1991). Hope fault, Jordan thrust, and uplift of the seaward Kaikoura Range, New Zealand. *Geology*, 19(4), 393–396. [https://doi.org/10.1130/0091-7613\(1991\)019<0393:HFJTAU>2.2.CO;2](https://doi.org/10.1130/0091-7613(1991)019<0393:HFJTAU>2.2.CO;2)
- Wallace, L. M., Barnes, P., Beavan, J., Van Dissen, R., Litchfield, N., Mountjoy, J., et al. (2012). The kinematics of a transition from subduction to strike-slip: An example from the central New Zealand plate boundary. *Journal of Geophysical Research*, 117, B02405. <https://doi.org/10.1029/2011JB008640>
- Wallace, R. E. (1987). Grouping and migration of surface faulting and variations in slip rates on faults in the Great Basin province. *Bulletin of the Seismological Society of America*, 77(3), 868–876. <https://doi.org/10.1029/2008RG000260.0>
- Weldon, R., Scharer, K., Fumal, T., & Biasi, G. (2004). Wrightwood and the earthquake cycle: What a long recurrence record tells us about how faults work. *GSA Today*, 14(9), 4. <https://doi.org/10.1130/1052-5173>
- Zinke, R., Dolan, J. F., Rhodes, E. J., Van Dissen, R., & McGuire, C. P. (2017). Highly variable latest Pleistocene–Holocene incremental slip rates on the Awatere fault at Saxton River, South Island, New Zealand, revealed by lidar mapping and luminescence dating. *Geophysical Research Letters*, 44, 11,301–11,310. <https://doi.org/10.1002/2017GL075048>
- Zinke, R., Dolan, J. F., Van Dissen, R., Grenader, J. R., Rhodes, E. J., McGuire, C. P., et al. (2015). Evolution and progressive geomorphic manifestation of surface faulting: A comparison of the Wairau and Awatere faults, South Island, New Zealand. *Geology*, 43(11), 1019–1022. <https://doi.org/10.1130/G37065.1>